JOURNAL OF BONE AND MINERAL RESEARCH
Volume 24, Number 11, 2009
Published online on May 4, 2009; doi: 10.1359/JBMR.090507

Enhanced Osteoclastogenesis Causes Osteopenia in Twisted Gastrulation-Deficient Mice Through Increased BMP Signaling

Julio E. Sotillo Rodriguez,[1] Kim C. Mansky,[2] Eric D. Jensen,[1] Ann E. Carlson,[1] Toni Schwarz,[2] Lan Pham,[2] BreAnne MacKenzie,[3] Hari Prasad,[1,4] Michael D. Rohrer,[1,4] Anna Petryk,[3,5] and Rajaram Gopalakrishnan[1]

ABSTRACT: The uncoupling of osteoblastic and osteoclastic activity is central to disorders such as osteoporosis, osteolytic malignancies, and periodontitis. Numerous studies have shown explicit functions for bone morphogenetic proteins (BMPs) in skeletogenesis. Their signaling activity has been shown in various contexts to be regulated by extracellular proteins, including Twisted gastrulation (TWSG1). However, experimental paradigms determining the effects of BMP regulators on bone remodeling are limited. In this study, we assessed the role of TWSG1 in postnatal bone homeostasis. *Twsg1*-deficient (*Twsg1*$^{-/-}$) mice developed osteopenia that could not be explained by defective osteoblast function, because mineral apposition rate and differentiation markers were not significantly different compared with wildtype (WT) mice. Instead, we discovered a striking enhancement of osteoclastogenesis in *Twsg1*$^{-/-}$ mice, leading to increased bone resorption with resultant osteopenia. Enhanced osteoclastogenesis in *Twsg1*$^{-/-}$ mice was caused by increased cell fusion, differentiation, and function of osteoclasts. Furthermore, RANKL-mediated osteoclastogenesis and phosphorylated Smad1/5/8 levels were enhanced when WT osteoclasts were treated with recombinant BMP2, suggesting direct regulation of osteoclast differentiation by BMPs. Increase in detectable levels of phosphorylated Smad 1/5/8 was noted in osteoclasts from *Twsg1*$^{-/-}$ mice compared with WT mice. Furthermore, the enhanced osteoclastogenesis in *Twsg1*$^{-/-}$ mice was reversed in vitro in a dose-dependent manner with exposure to Noggin, a BMP antagonist, strongly suggesting that the enhanced osteoclastogenesis in *Twsg1* mutants is attributable to increased BMP signaling. Thus, we present a novel and previously uncharacterized role for TWSG1 in inhibiting osteoclastogenesis through regulation of BMP activity.
J Bone Miner Res 2009;24:1917–1926. Published online on May 4, 2009; doi: 10.1359/JBMR.090507

Key words: osteoclast, osteoblast, Twisted gastrulation, bone morphogenetic protein, resorption, bone, osteopenia

Address correspondence to: *Rajaram Gopalakrishnan, BDS, PhD, Department of Diagnostic and Biological Sciences, University of Minnesota School of Dentistry, 16-108A Moos Tower, 515 Delaware Street SE, Minneapolis, MN 55455, USA, E-mail: gopal007@umn.edu*

INTRODUCTION

THE DYNAMIC NATURE of bone remodeling maintains the integrity of bone tissue throughout life.[1] Osteoblasts and osteoclasts serve as integral components of bone remodeling. New bone matrix is synthesized, deposited, and mineralized by mesenchymal-derived osteoblasts. Conversely, osteoclasts, derived from hematopoietic stem cells, mediate the removal of old bone and facilitate the systemic maintenance of mineral homeostasis. When osteoblastic and osteoclastic activity become uncoupled, pathological conditions arise that are associated with decreased skeletal integrity,[1] such as osteoporosis, osteolytic malignancies, and periodontitis. Individuals afflicted with such diseases experience deterioration of bone tissue, resulting in increased bone fragility, susceptibility to fractures, bone pain, and periodontal bone loss. These clinical consequences represent a global health concern; hence, there is a great need for experimental systems that will study molecular signals that mediate skeletal remodeling.

Osteoblasts and osteoclasts are both subject to paracrine and autocrine regulation mediated by numerous cytokines and growth factors. Although bone morphogenetic proteins (BMPs) are indispensable for osteoblast differentiation and function, controversy exists regarding their role in osteoclast activation.[2,3] As reviewed by Giannoudis et al.,[4] the limited data available show both positive and negative influences of BMPs on osteoclasts. Furthermore, it remains unclear whether BMP effects on osteoclast precursors are direct or are mediated indirectly by osteoblasts through altered expression of RANKL and osteoprotegerin (OPG). Evidence for the role of BMPs in

The authors state that they have no conflicts of interest.

[1]Department of Diagnostic and Biological Sciences, University of Minnesota School of Dentistry, Minneapolis, Minnesota, USA; [2]Department of Developmental and Surgical Sciences, University of Minnesota School of Dentistry, Minneapolis, Minnesota, USA; [3]Department of Pediatrics, University of Minnesota Medical School, Minneapolis, Minnesota, USA; [4]Hard Tissue Research Laboratory, University of Minnesota School of Dentistry, Minneapolis, Minnesota, USA; [5]Department of Genetics, Cell Biology and Development, University of Minnesota, Minneapolis, Minnesota, USA.

osteoclast function was provided by Mishina et al.,[5] where 10-mo-old mice harboring an osteoblast-specific BMP receptor type IA gene ablation showed a decrease in osteoclastic bone resorption.[5] This has led to the speculation that loss of BMP signaling in osteoblasts leads to impairment of osteoclast-supporting activities, causing downregulation of osteoclast function as the mice age. The interactions between BMPs and osteoclast were shown by Abe et al.,[6] when they reported that Noggin, a BMP antagonist, dose-dependently inhibited osteoclast formation in co-culture experiments showing that Noggin's effect was indirect through stromal cells. Apart from the indirect regulation of osteoclasts, several reports have indicated that osteoclasts express BMP receptors and that BMPs directly stimulate osteoclast differentiation in vitro.[7–9] Osteoclast differentiation supported by colony-stimulating factor-1 (CSF-1) and RANKL is enhanced in the presence of BMPs. Kaneko et al.[9] further showed that BMP2 can directly stimulate pit formation even in the absence of exogenous RANKL. Itoh et al.[7] showed that osteoclast progenitors expressed endogenous BMP2; however, they noted that RANKL was essential for BMP2 stimulation of osteoclastogenesis. Recently, Okamoto et al.[10] showed decreased osteoclast number and reduced osteoclastic bone resorption in mice overexpressing Noggin, a well-documented extracellular BMP antagonist, specifically in osteoblasts using a 2.3-kb *Col1A1* promoter. The authors also showed that the impaired osteoclast formation caused by Noggin overexpression was rescued by BMP2 administration in vitro. This suggested that Noggin inhibits osteoclast activity through attenuating BMP signaling. The authors furthermore showed increased Smad 1/5/8 phosphorylation in osteoclast precursor cells after BMP2 treatment. Feeley et al.,[11] in a recent study, showed that Noggin decreased PC-3 prostate cancer cell–induced bone resorption in a bone tumor model, suggesting a regulatory function for BMPs on osteoclasts.

BMPs exert their biological activities by signaling through type I and II serine/threonine kinase transmembrane receptors.[7,12,13] This signaling is subject to precise regulation at the intracellular and extracellular levels.[14,15] Intracellular regulation occurs through inhibition of Smad-mediated signaling cascades by inhibitory Smads and Smad ubiquitination inhibitory factors.[16–18] Extracellular modulation occurs through several secreted proteins such as Noggin, Chordin, and Twisted gastrulation (TWSG1) that physically interact and limit accessibility of BMPs to their cell surface receptors.[14,19] *Twsg1*, originally identified in *Drosophila*, encodes a 23.5-kDa glycoprotein that is expressed by numerous cell types, including osteoblasts, and as shown for the first time in this report, by osteoclasts (Figs. 6A–6C).[20–22] In addition to its BMP antagonism, TWSG1 also exhibits BMP agonist activity depending on the stage of development or concentration of interacting proteins in various species.[23–28]

We generated *Twsg1*-deficient mice in two different pure backgrounds: C57BL/6 and 129Sv/Ev. *Twsg1*$^{-/-}$ mice in C57BL/6 background have severe craniofacial defects and show high perinatal mortality, limiting the study of the postnatal bone formation.[29] These mice exhibit pronounced forebrain defects (holoprosencephaly) and a spectrum of craniofacial defects that stem from abnormal morphogenesis and increased apoptosis in the first branchial arch as early as E9.5.[30] On the other hand, *Twsg1*$^{-/-}$ mice in the pure 129Sv/Ev background, which were used in this study, are viable and fertile with a very low frequency of craniofacial defects.

The goal of this study was to assess the role of TWSG1 in postnatal bone homeostasis and its importance in the regulation of cellular activity sustaining bone remodeling. Because survival of *Twsg1*$^{-/-}$ mice depends largely on genetic background, we chose mice in the 129/SvEv background, based on our previous observation that the majority of mutant mice in this background survive to adulthood.[29]

MATERIALS AND METHODS

Mice

Twsg1$^{-/-}$ mice were generated and genotyping performed as previously described.[29] Briefly, *Twsg1*-heterozygous (*Twsg1*$^{+/-}$) 129Sv/Ev mice were bred to obtain WT and *Twsg1*$^{-/-}$ mice. Animals were killed by CO_2 inhalation. Use and care of the mice in this study was approved by the University of Minnesota Institutional Animal Care and Use Committee.

Radiographic and μCT analyses

We performed X-ray analysis of femurs from *Twsg1*$^{-/-}$ and WT mice using a Specimen Radiography System Model MX-20 (Faxitron X-ray). μCT analysis was performed at MicroCT Facility and Micromechanics Laboratory, University of Connecticut Health Center, Farmington, CT, USA.

Primary osteoblast cultures

Primary osteoblasts were isolated as previously described.[31] Calvaria from 7- to 10-day-old WT or *Twsg1*$^{-/-}$ mice were dissected and subjected to sequential digestions with 2 mg/ml of collagenase A (Roche Molecular Biomedicals) in MEM solution containing 0.25% trypsin (Gibco) for 20, 40, and 90 min. The third digestion was plated at 1.5×10^4 cells/cm^2. Cells were maintained at 37°C in a humidified atmosphere of 5% CO_2, in MEM media containing 10% FBS, 1% penicillin/streptomycin, and 1% nonessential amino acids. On confluency, cells were differentiated with ascorbic acid (50 μg/ml)–containing media (Sigma-Aldrich).

Primary osteoclast cultures and CD11b-enrichment

Primary osteoclast cultures were prepared from bone marrow and spleen of WT or *Twsg1*$^{-/-}$ mice as previously described.[32] Spleens and bone marrow flushed from femurs were isolated and mechanically dissociated. Resulting cells were cultured for 3 days in the presence of 50 ng/ml CSF-1 on non–tissue culture dishes. The adherent cell population, containing the committed osteoclast precursors, was cultured for the indicated amount of time with

TABLE 1. Real-Time PCR Primer Sequences

Gene	*Forward*	*Reverse*
Osteocalcin	GAACAGACTCCGGCGCTA	AGGGAGGATCAAGTCCCG
Alkaline Phosphatase	GCTGATCATTCCCACGTTTT	CTGGGCCTGGTAGTTGTTGT
RANKL	AGCCGAGACTACGGCAAGTA	GCGCTCGAAAGTACAGGAAC
Osteoprotegerin	CTGCCTGGGAAGAAGATCAG	TTGTGAAGCTGTGCAGGAAC
Twisted gastrulation	TGAGCAAATGCCTCATTCAG	GGTTGCACATACCGACACAG
Noggin	AAGAAGCTGAGGAGGAAGTT	GACTTGGATGGCTTACACAC
Chordin	GGTCAGCTGCAAGAACATCA	GGTTCCCCTCGATCACTGTA
NFATc1	TCATCCTGTCCAACACCAAA	TCACCCTGGTGTTCTTCCTC
Cathepsin K	AGGGAAGCAAGCACTGGATA	GCTGGCTGGAATCACATCTT
TRACP	CGTCTCTGCACAGATTGCA	GAGTTGCCACACAGCATCAC
DCSTAMP	GGGCACCAGTATTTTCCTGA	TGGCAGGATCCAGTAAAAGG
GAPDH	TGCACCACCAACTGCTTAG	GATGCAGGGATGATGTTC
L4	CCTTCTCTGGAACAACCTTCTCG	AAGATGATGAACACCGACCTTAGC

All sequences are 5′-3′.

indicated amounts of CSF-1 (R&D Systems) and RANKL (R&D Systems). Osteoclast resorption ability was assessed on dentine discs (Immunodiagnostic Systems).

CD11b enrichment of osteoclast precursor cells was performed after culturing the cells for 3 days in 50 ng/ml CSF-1 according to manufacturer's instructions (Miltenyi Biotec). Briefly, 1×10^7 bone marrow cells were resuspended in 90 μl of magnetic cell sorting (MACS) buffer (2 mM EDTA, 0.5% BSA in PBS) and incubated with 20 μl of $CD11b^+$ microbeads for 20 min on ice. Cells/beads mixture were mixed every 5 min. After cells were brought up to a volume of 2 ml using MACS buffer (2 ml/1×10^7 cells), 100 μl of cells was removed for fluorescence activated cell sorter (FACS) analysis. Cells were pelleted and resuspended in 500 μl MACS buffer/1×10^8 cells. Supernatants were saved after placement of the columns in a magnetic field. After removal of a wash sample for FACS analysis, the remaining fraction of magnetically labeled cells were resuspended in 5 ml of MACS buffer and flushed from the column. A small fraction of the eluate was saved for FACS analysis. Cells were counted and equal number of cells were plated for osteoclast differentiation and resorption assays.

Histology and dynamic histomorphometric analysis

Histological sections from 1-mo-old decalcified mouse femurs and primary osteoclast cultures were stained for TRACP activity using a commercially available kit (Sigma-Aldrich). TWSG1 protein in osteoclast cultures was detected by immunofluorescence using rat anti-mouse Twsg1 antibody (R&D Systems) at 1:200 dilution according to method described previously.[32] Dynamic histomorphometry was assessed by double-label procedure (two injections of 25 mg/kg tetracycline [Sigma-Aldrich] 5 days apart), and undecalcified sections were analyzed by Osteomeasure system (OsteoMetrics) and NIH ImageJ.[33,34]

Serum bone formation and resorption markers

Blood was collected from WT and *Twsg1*$^{-/-}$ mice and used to determine serum levels of TRACP, osteocalcin (OCN), and OPG by ELISA (SBA Sciences, TRACP; BTI Biomedical Technologies, OCN; Alpco, OPG).

Proliferation

Osteoclast proliferation was assessed by CellTiter 96 AQueous One Solution Cell Proliferation kit (Promega) according to the manufacturer's instructions.

Quantitative real-time PCR

Status of cellular differentiation was assessed by real-time RT-PCR. Total RNA was isolated from cells using TRIzol reagent (Invitrogen Life Technologies) and quantitated by UV spectroscopy. RT was performed using 1 μg of RNA and the iScript cDNA Synthesis kit (Bio-Rad). Quantitative real-time RT-PCR was performed using a Mx 3000P QPCR System (Stratagene) for osteoblast analysis and MyiQ Single-Color Real-Time PCR Detection System (Bio-Rad) for osteoclast analysis, using 1 μl of the cDNA with 1× Brilliant SYBR Green master mix (osteoblast) or 2× iQ SYBR Green supermix (osteoclast) (Stratagene and Bio-Rad, respectively). Osteoblast genes were normalized to *Gapdh* mRNA, and osteoclast genes were normalized to *L4* mRNA. Primer sequences for all genes analyzed are provided in Table 1. The sequences were designed using Primer3[35] or obtained from previous publications.[36]

in situ hybridization

Mouse *Twsg1* probes were generated from a 214-bp cDNA fragment (256–469 bp of the coding sequence; GenBank NM023053) subcloned into pCR II TOPO vector (Invitrogen). To generate the antisense probe, the plasmid was linearized with *Bam*HI and transcribed with T7, and to generate the sense probe, the plasmid was linearized with *Not*I and transcribed with SP6 polymerase using the Maxiscript kit (Ambion) and labeled with digoxigenin RNA labeling mixture (Roche). Hybridization was performed as previously described,[37] and the *Twsg1* mRNA signal was detected with BM Purple (Roche) following the manufacturer's instructions. Photomicrographs were taken with a Nikon Eclipse 50i microscope, and the images were captured using SPOT imaging software (Diagnostics Instruments).

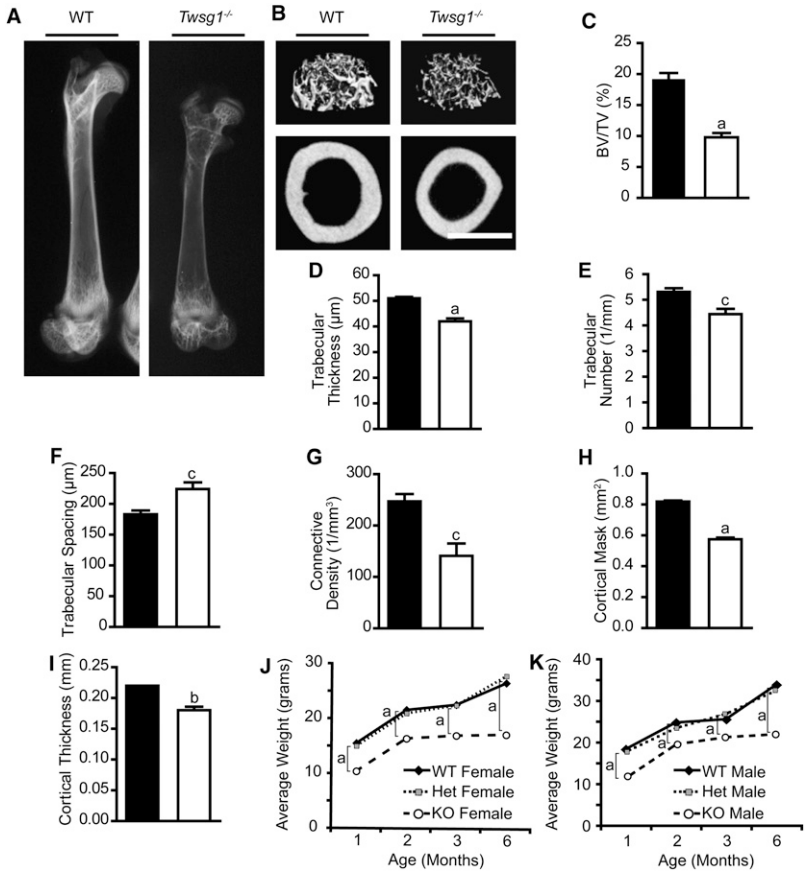

FIG. 1. Bone phenotype of *Twsg1*$^{-/-}$ mice. (A) Representative faxitron image from 1-mo-old WT and *Twsg1*$^{-/-}$ mouse femurs. (B) Representative μCT images from 3-mo-old WT and *Twsg1*$^{-/-}$ female mouse femurs. Trabecular bone is shown in top panels and cortical bone is shown in bottom panels (scale bar = 1 mm). Static histomorphometric parameters reflecting trabecular and cortical bone integrity from WT (■; $n = 3$) and *Twsg1*$^{-/-}$ (□; $n = 3$) bones, including (C) bone volume fraction, (D) trabecular thickness, (E) trabecular number, (F) trabecular spacing, (G) connective density, (H) cortical mask, and (I) cortical thickness. (J and K) Average body weight measurements of WT, heterozygote, and *Twsg1*$^{-/-}$ females and males, respectively. $^{a}p < 0.05$; $^{b}p < 0.005$; $^{c}p < 0.001$.

Western blotting

Western blot analysis was performed to determine phosphorylated Smad 1/5/8 levels in primary osteoclasts differentiated in the presence of 60 ng/ml RANKL for 3 days. Whole cell extracts were prepared by lysing cells in modified RIPA buffer supplemented with phosphatase (Roche) and protease (Sigma-Aldrich) inhibitors. To prepare nuclear extracts, cells were collected in PBS and lysed in ice for 5 min in Iso-Hi Buffer (10 mM Tris, pH 7.8, 140 mM NaCl, 1.5 mM $MgCl_2$, 0.5% NP-40) supplemented with protease and phosphatase inhibitor cocktails. Nuclei were pelleted by centrifugation at 5000 rpm and resuspended in SDS-PAGE loading buffer. Proteins were resolved by SDS-PAGE, transferred to PVDF membrane (Millipore), and immunoblotted with rabbit anti-phosphorylated Smad 1/5/8 (1:1000; catalog 9511; Cell Signaling) antibody, anti-total Smad 1/5/8 antibody (1:1000; catalog SC-6031R; Santa Cruz), or anti-actin antibody (1:5000, catalog SC-1616; Santa Cruz) and appropriate horseradish peroxidase–conjugated secondary antibodies (1:10,000; Santa Cruz). Immunoreactive bands were visualized using ECL Plus substrate (GE Health Systems).

Statistical analysis

All statistical analyses were performed using Prism 4 (Graphpad Software). Real-time RT-PCR analysis is reported as the mean ± SD of triplicate independent RNA samples. All experiments were repeated three times. ANOVA and Student's *t*-test were used to assess significance between groups (NS = not significant; $^{a}p < 0.05$; $^{b}p < 0.005$; $^{c}p < 0.001$).

RESULTS

Deficiency in Twsg1 results in severe osteopenia

Radiographic analysis showed that *Twsg1*$^{-/-}$ mice were osteopenic at 1 (Fig. 1A), 3 (data not shown), and 6 mo (data not shown). μCT analysis (Fig. 1B), which shows the integrity of trabecular and cortical morphology, showed 49% reduction in bone volume fraction (BV/TV) of *Twsg1*$^{-/-}$ mice compared with WT mice at 3 mo (Fig. 1C). Reduced cancellous bone was apparent, because femurs from *Twsg1*$^{-/-}$ mice showed decreased trabecular thickness (Fig. 1D) and trabecular number (Fig. 1E), increased trabecular spacing (Fig. 1F), and reduced connectivity density (Fig. 1G). Similarly, cortical bone was also severely reduced, because femurs from *Twsg1*$^{-/-}$ mice showed decreased cortical area (Fig. 1H) and cortical thickness (Fig. 1I). Although μCT analysis was performed only on 3-mo-old females, X-ray analysis clearly showed reduced bone mass at 1 and 6 mo (data not shown). Furthermore, X-ray analysis clearly showed that both male and female *Twsg1*$^{-/-}$ mice exhibited a similar reduction in bone mass compared with WT mice (data not shown). As shown in Figs. 1J and 1K,

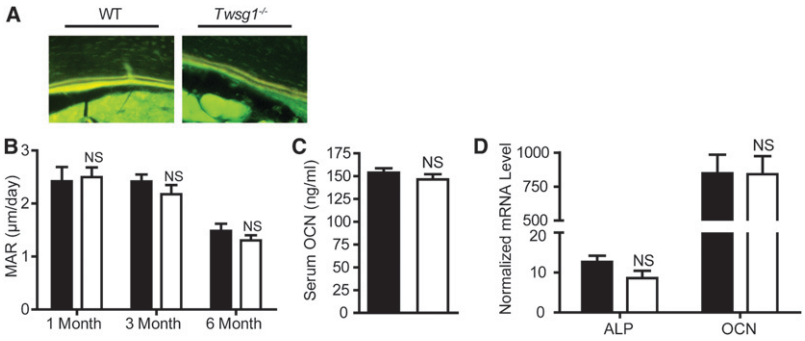

FIG. 2. In vivo and in vitro characterization of osteoblast function from WT and *Twsg1*$^{-/-}$ mice. WT and *Twsg1*$^{-/-}$ mice were injected 5 days apart with 25 mg/kg tetracycline (n = 7–11). (A) Representative fluorescent images from 3-mo-old WT and *Twsg1*$^{-/-}$ femurs. (B) Mineral apposition rate (MAR) of 1-, 3-, and 6-mo-old WT and *Twsg1*$^{-/-}$ mice. (C) Serum OCN measured by ELISA. (D) Expression profile of *Alp* and *Ocn* mRNA from 8-day osteoblast cultures. WT (■); *Twsg1*$^{-/-}$ (□). NS, not significant.

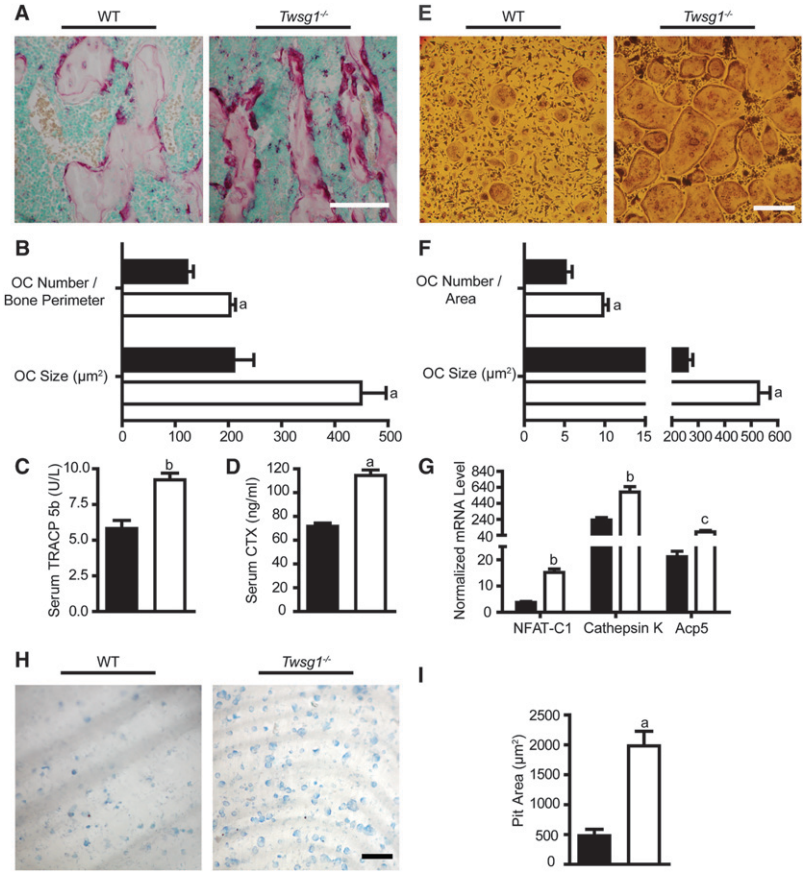

FIG. 3. In vivo and in vitro characterization of osteoclast function from WT and *Twsg1*$^{-/-}$ mice. (A) TRACP-stained bone sections from WT and *Twsg1*$^{-/-}$ femurs (scale bar = 200 μm). (B) Histomorphometric analysis of TRACP-stained bone sections from WT and *Twsg1*$^{-/-}$ femurs. (C) Serum TRACP 5b measured by ELISA. (D) Serum CTX measured by ELISA. (E) TRACP-stained osteoclasts after differentiation after 7 days in culture of CD11b-enriched bone marrow cultures (scale bar = 200 μm). (F) Histomorphometric analysis of TRACP-stained osteoclasts. (G) Expression profile of *NFAT-C1*, *cathepsin K*, and *Acp5* (encoding TRACP) mRNA from 3-day osteoclast cultures. (H) Representative photomicrograph of toluidine blue–stained resorption pits on dentine discs (scale bar = 200 μm). (I) Quantitation of resorption pit area. WT (■); *Twsg1*$^{-/-}$ (□). $^{a}p < 0.05$; $^{b}p < 0.005$; $^{c}p < 0.001$.

both female and male *Twsg1*$^{-/-}$ mice showed significantly reduced body weights compared with WT and heterozygous mice at 1-, 3-, and 6-mo time points.

Osteopenia in Twsg1$^{-/-}$ *mice is not caused by a defect in osteoblast function*

To determine whether osteopenia in *Twsg1*$^{-/-}$ mice was caused by reduced osteoblast function, in vivo and in vitro indices of bone formation were determined. The mineral apposition rates of 1-, 3-, and 6-mo-old *Twsg1*$^{-/-}$ mice were not significantly different from age-matched WT mice (Figs. 2A and 2B). Correspondingly, levels of serum OCN, a marker of osteoblast function, were indistinguishable between the two genotypes (Fig. 2C). In vitro studies using WT and *Twsg1*$^{-/-}$ primary calvarial osteoblasts showed no differences in mRNA expression of the osteoblast markers alkaline phosphatase (*Alp*) and *Ocn* (Fig. 2D). Therefore, consistent with a previous report, we found no impairment in osteoblast function in *Twsg1*$^{-/-}$ mice.[38]

Osteopenia in Twsg1$^{-/-}$ *mice results from enhanced osteoclast maturation and function*

Because osteoblast function did not explain the osteopenic phenotype, we next examined whether deficiency of *Twsg1* alters bone resorption. As shown in Figs. 3A and 3B, bone sections from *Twsg1*$^{-/-}$ mice showed an increase in

number and size of TRACP$^+$ multinucleated osteoclasts relative to WT mice. Similarly, levels of serum TRACP 5b (a marker of osteoclast number; Fig. 3C) and carboxy-terminal collagen cross-links (CTX: a marker of collagen degradation indicative of bone resorption; Fig. 3D) were higher in *Twsg1*$^{-/-}$ mice relative to WT mice.

The in vivo osteoclast phenotype of *Twsg1*$^{-/-}$ mice correlated with in vitro experiments using CD11b-enriched bone marrow osteoclast precursors. CD11b enrichment experiments were performed to select for osteoclast precursors of monocyte/macrophage lineage without contamination with stromal cells. As shown in Figs. 3E and 3F, relative to WT osteoclast cultures, multinucleated TRACP$^+$ osteoclasts from *Twsg1*$^{-/-}$ mice were increased in number and size when allowed to differentiate in the presence of 60 ng/ml RANKL and 10 ng/ml CSF-1. Additionally, *Twsg1*$^{-/-}$ osteoclasts exhibited increased mRNA expression of differentiation genes, nuclear factor of activated T-cells-C1 (*Nfat-c1*; 3.6-fold), Cathepsin K (2.4-fold), and acid phosphatase 5 (*Acp5,* which encodes TRACP; 4.5-fold; Fig. 3G). Consistent with increased serum CTX levels, *Twsg1*$^{-/-}$-derived osteoclasts cultured on dentine discs showed increased resorption pit area relative to WT osteoclasts (Figs. 3H and 3I). Similar results were obtained when in vitro experiments were repeated using osteoclast precursors from spleen (data not shown). Our data showed for the first time that the osteopenic phenotype observed in *Twsg1*-deficient mice occurs as a direct result of increased formation, differentiation, and function of multinucleated osteoclasts.

Enhanced osteoclast phenotype in Twsg1$^{-/-}$ *mice is mediated by increased cell–cell fusion*

We next examined whether the enhanced osteoclastogenesis in *Twsg1*$^{-/-}$ mice was caused by increased proliferation and/or fusion of osteoclast precursors. As shown in Fig. 4A, osteoclast precursors from *Twsg1*$^{-/-}$ mice did not show increased proliferation compared with WT mice. Although the total number of nuclei was not significantly different (Fig. 4B), osteoclasts from *Twsg1*$^{-/-}$ mice contained significantly more nuclei per multinucleated cell (1.6-fold, $p < 0.005$) than osteoclasts from WT animals (Fig. 4C), suggesting that the increased osteoclastogenesis in *Twsg1*$^{-/-}$ mice results from enhanced fusion of osteoclast precursors rather than enhanced proliferation. Increased fusion in *Twsg1*$^{-/-}$ mice was further evidenced by a concomitant 13-fold ($p < 0.005$) increase in expression of dendritic cell–specific transmembrane protein (DC-STAMP) mRNA, encoding a key protein necessary for cell fusion (Fig. 4D).[39]

Expression of RANKL and OPG by osteoblasts is unaffected in Twsg1$^{-/-}$ *mice*

Osteoclast maturation is regulated by osteoblasts through secretion of the RANKL and its decoy receptor OPG.[1,40] Our results showed that serum OPG levels (WT = 2.084 ± 0.101 pM; *Twsg1*$^{-/-}$ = 2.181 ± 0.186 pM) and fold expression of RANKL (WT = 0.202 ± 0.086; *Twsg1*$^{-/-}$ = 0.189 ± 0.104) and OPG (WT = 0.807 ± 0.225; *Twsg1*$^{-/-}$ = 0.760 ± 0.310) in primary osteoblast cultures were not significantly different in *Twsg1*$^{-/-}$ mice relative to WT mice. These results showed that the osteopenia observed in *Twsg1*$^{-/-}$ mice cannot be explained by an increased ability of osteoblasts to stimulate osteoclastogenesis.

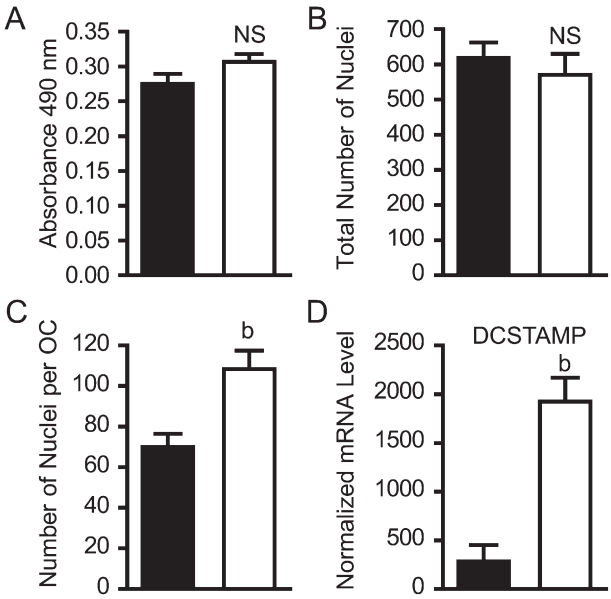

FIG. 4. Regulation of enhanced osteoclastogenesis by increased cell–cell fusion. (A) Cell proliferation assay. Day 5 osteoclast cultures were DAPI stained, and histomorphometry was performed to assess the total number of nuclei (B) and the total number of nuclei per multinucleated cell (C) within 0.25 of a 2-cm^2 dish. (D) Expression profile of DC-STAMP mRNA from day 3 osteoclast cultures. WT (■); *Twsg1*$^{-/-}$ (□). NS, not significant. $^b p < 0.005$.

BMP signaling regulates enhanced osteoclastogenesis

Because TWSG1 specifically regulates BMP signaling, we studied whether the observed increase in osteoclastogenesis in *Twsg1*$^{-/-}$ mice was caused by altered BMP activity. Osteoclast precursors derived from WT or *Twsg1*$^{-/-}$ mice were treated with 60 ng/ml RANKL for 3 days. Nuclear protein extracts were used for detection of phosphorylated Smad1/5/8 by Western blot analysis. We detected an increase in phosphorylated Smad1/5/8 levels in *Twsg1*$^{-/-}$ osteoclasts compared with WT osteoclasts (Fig. 5A). Furthermore, we observed a dose-dependent attenuation of osteoclast size and number (Figs. 5B–5D) in cultures containing Noggin, a specific BMP-2 and -4 antagonist,[41] showing that the phenotype in *Twsg1*$^{-/-}$ osteoclasts is caused by enhanced BMP signals received by the *Twsg1*$^{-/-}$ osteoclast precursors and that TWSG1 acts as a BMP antagonist during normal osteoclast maturation. To further understand the functional significance of TWSG1, we studied its expression in osteoclasts relative to Noggin and Chordin. Real-time RT-PCR analysis showed that *Twsg1* mRNA was expressed in osteoclasts at significantly higher levels than Noggin or Chordin (Fig. 6A). Immunofluorescence localization confirmed the expression

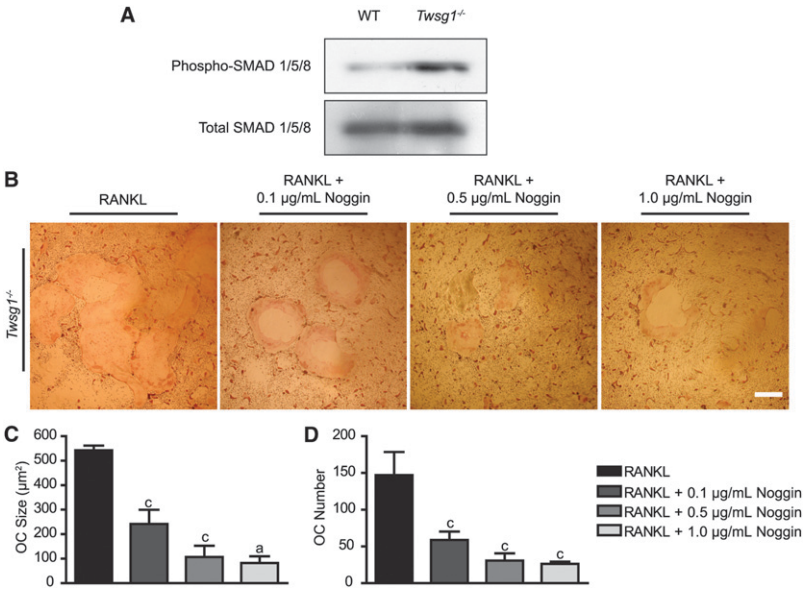

FIG. 5. BMP signaling is associated with enhanced osteoclastogenesis in *Twsg1*$^{-/-}$ mice. (A) Representative Western blots of nuclear proteins from WT and *Twsg1*$^{-/-}$ osteoclast cultures differentiated with RANKL (60 ng/ml) for 3 days and immunoblotted against phospho- and total- SMADs1/5/8. (B) TRACP staining (scale bar = 200 μm) and histomorphometry (C and D) from 7 day *Twsg1*$^{-/-}$ osteoclast cultures treated with or without Noggin (0.1, 0.5, and 1.0 μg/ml). $^{a}p < 0.05$; $^{c}p < 0.001$.

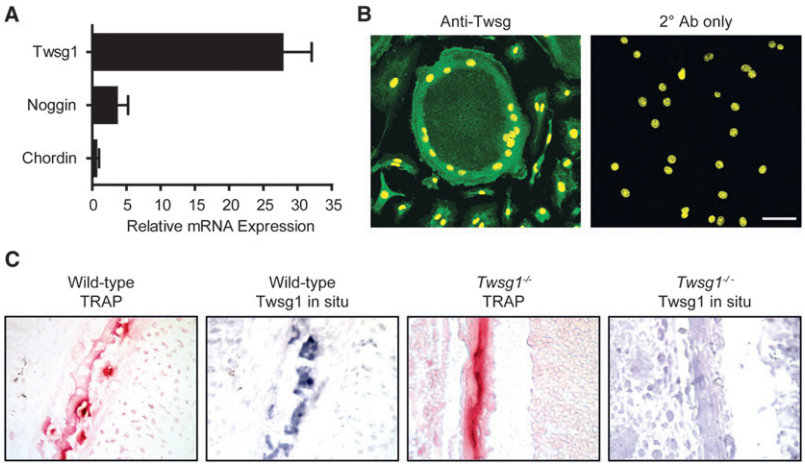

FIG. 6. Expression of Twsg1 in WT and *Twsg1*$^{-/-}$ osteoclasts. (A) Real-time RT-PCR analysis of day 5 osteoclasts for expression of TWSG1, Noggin, and Chordin. (B) Twsg1 immunofluorescence staining (green) of day 5 osteoclast cultures counterstained with DAPI (yellow). Secondary-antibody only negative control is represented in the right panel (scale bar = 50 μm). (C) In situ hybridization showing absence of *Twsg1* mRNA in calvarial sections of 1-day-old *Twsg1*$^{-/-}$ mice. TRACP staining of respective serial sections identifies the osteoclasts.

of TWSG1 in osteoclasts (Fig. 6B). It seems that the protein was localized primarily to the cell membrane, which would be consistent with its regulatory function toward BMPs. Furthermore, expression of BMP2 and its receptors were detected by real-time RT-PCR in WT osteoclasts as previously shown by others[9,42] (data not shown). To confirm the absence of *Twsg1* mRNA in osteoclasts from *Twsg1*$^{-/-}$ mice, a nonradioactive in situ hybridization was used (Fig. 6C). Hybridization with antisense probe to *Twsg1* showed a positive signal in 1-day-old WT calvaria. Conversely, *Twsg1* mRNA was not detected in calvarial sections from 1-day-old *Twsg1*$^{-/-}$ mice. TRACP staining of serial sections from the same animals were used to localize the osteoclasts. No signal was obtained in sections hybridized with *Twsg1* sense probe, which was used as a negative control (data not shown).

To determine whether BMPs could directly activate differentiation of WT osteoclast precursors into multinuclear TRACP^{+} cells, we examined differentiation of WT osteoclast precursors in the presence of 30 ng/ml of BMP2 and suboptimal levels of RANKL (30 ng/ml). We found significantly increased numbers of and larger-sized TRACP^{+} multinucleated osteoclasts relative to WT osteoclast precursors exposed only to RANKL (30 ng/ml; Figs. 7A and 7B). Osteoclast precursors that were treated with BMP2 alone did not undergo differentiation, because no TRACP^{+} mononuclear or multinuclear cells were observed (data not shown). We next examined whether BMP2 increases levels of phosphorylated Smad1/5/8 in WT osteoclasts. WT spleen and bone marrow–derived osteoclasts were cultured in the presence of 60 ng/ml RANKL for 3 days, after which primary osteoclasts or MC3T3-E1 pre-osteoblasts, which were used as positive control, were treated with recombinant human BMP2 (R&D Systems) at 100 ng/ml for 30 min. As shown in Fig. 7C, phosphorylated Smad1/5/8 levels were increased in cultures treated with BMP2 compared with RANKL-treated cultures alone. These results show that BMP2 can increase phosphorylated

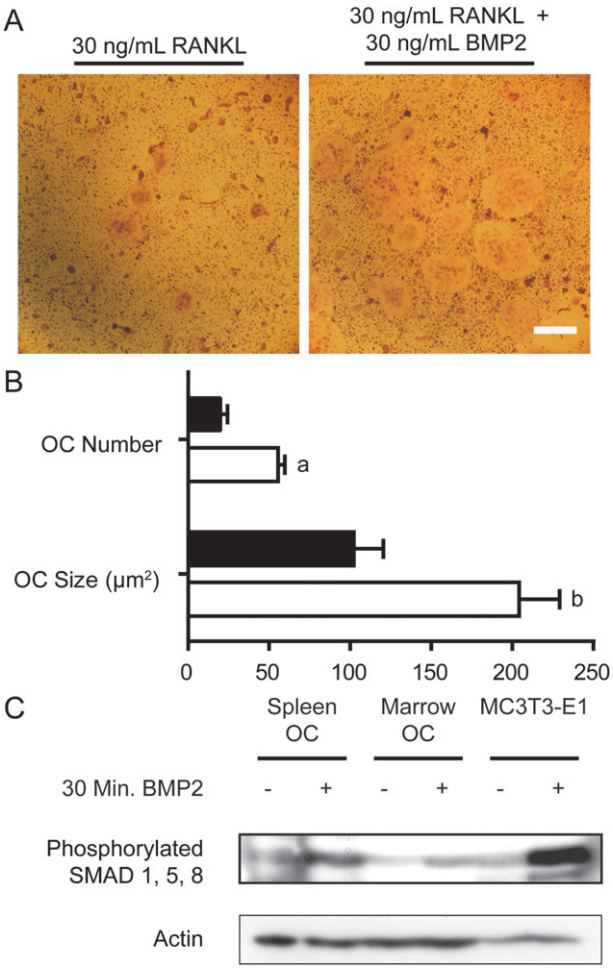

FIG. 7. BMP2 directly enhances RANKL-stimulated osteoclastogenesis and pSmad1/5/8 levels in primary osteoclasts. (A) TRACP staining and (B) histomorphometry from 7-day WT osteoclast cultures differentiated with half-optimal levels of RANKL (30 ng/ml) treated with or without 30 ng/ml of BMP2 [RANKL 30 ng/ml (■); RANKL 30 ng/ml + BMP2 30 ng/ml (□)]. Scale bar = 200 μm. (C) Representative Western blots of nuclear proteins from primary spleen and bone marrow osteoclast cultures differentiated with RANKL (60 ng/ml) for 3 days and immunoblotted against phospho- and total-Smad 1/5/8. $^{a}p < 0.05$; $^{b}p < 0.005$.

Smad levels in primary osteoclasts and BMP signaling can enhance RANKL-mediated osteoclastogenesis and provide evidence for a positive direct regulatory role of BMPs in osteoclast formation.

DISCUSSION

In this study, we investigated the role of TWSG1 in bone using a mouse model that is deficient for the *Twsg1* gene. We showed that loss of Twsg1 caused profound osteopenia that could not be explained by decreased osteoblast function but rather was caused by enhanced osteoclastogenesis and increased bone resorption. We also showed that the enhanced osteoclastogenesis in *Twsg1*$^{-/-}$ mice was from increased BMP signaling and BMP2 can cooperate with RANKL to enhance WT osteoclast differentiation.

Osteopenia has previously been reported in other *Twsg1*-deficient mouse models.[38,43] Along with osteopenia, Nosaka et al.[43] reported severe growth retardation that was attributed primarily to impaired cartilage differentiation and subsequent delayed endochondral bone formation in their *Twsg1*$^{-/-}$ mice. The osteopenia in the *Twsg1*$^{-/-}$ mouse model reported by Gazzero et al.[38] was transient, with 40% reduced trabecular bone volume at 4 wk but not at 7 wk. The authors did not see a defect in osteoblast or osteoclast function (the data to support the latter were not shown) and reported that the transient trabecular bone phenotype could be explained by a defect in endochondral bone formation. Our results are the first to show that enhanced osteoclastogenesis and increased bone resorption through increased BMP activity is a mechanism for osteopenia in mice deficient for *Twsg1*. This finding does not exclude a possibility of an additional cartilage defect also contributing to the skeletal phenotype.

Although the role of BMPs as potent inducers of osteoblast differentiation and ectopic bone formation has been well studied, only recently has the involvement of BMPs in osteoclast maturation and function been studied.[4] As reviewed in the Introduction, several reports have provided evidence for the role of BMPs in osteoclast function by either directly regulating osteoclasts or modifying osteoclast-supporting activities of osteoblasts. Our data showed that osteoclast differentiation sustained by RANKL is directly enhanced in the presence of BMP2 or the absence of TWSG1, which acts as a BMP inhibitor in osteoclasts. We provide evidence that the levels of phosphorylated Smad 1/5/8 are increased in osteoclast cultures from *Twsg1*$^{-/-}$ mice compared with WT cultures, consistent with an increase in BMP signaling. Likewise, the levels of phosphorylated Smad1/5/8 are increased in primary WT osteoclasts (both spleen and bone marrow derived) incubated with BMP2, further supporting direct activation of BMP signaling in osteoclasts.

It is intriguing that osteoblasts appeared unaffected in vivo, whereas our previously published in vitro experiments showed that TWSG1 could regulate osteoblast differentiation and function.[22] It is conceivable that other BMP antagonists such as Chordin and Noggin compensate for the lack of TWSG1 in osteoblasts in vivo, where their expression is abundant, but not in osteoclasts, where their levels are much lower relative to TWSG1. Spatiotemporal expression of BMP antagonists within the bone architecture or the degree to which these secreted proteins can diffuse to affect neighboring bone cells present alternative explanations that will be areas of future studies.

Our study has significant clinical implications because excessive osteoclast activity underlies loss of bone in osteoporosis, osteolytic bone tumors, and periodontitis. Whereas our studies focused on the deficiency of *Twsg1*, it remains to be determined whether administration of TWSG1 could inhibit excessive osteoclast function introducing a potential therapeutic approach for osteolytic diseases.

ACKNOWLEDGMENTS

We thank Dr. Douglas Adams University of Connecticut for μCT analysis, Margaret Ramnaraine (University of Minnesota) for assistance with CD11b isolation and FACS analysis, and Ashley Peterson and Lei Li (both at University of Minnesota) for assistance with laboratory procedures. We acknowledge the use of the confocal microscope made available through an NCRR Shared Instrumentation Grant (1 S10 RR16851). This project was supported in part by Academic Health Center Faculty Development Grant to R.G., R01 DE016601 to A.P., MinnCResT-T32 DE007288 to J.S.R. and L.P. from the National Institute of Dental and Craniofacial Research, and 3M Science and Technology Fellowship and Block grant from the University of Minnesota Graduate School to B.M.

REFERENCES

1. Zaidi M 2007 Skeletal remodeling in health and disease. Nat Med **13:**791–801.
2. Cao X, Chen D 2005 The BMP signaling and in vivo bone formation. Gene **357:**1–8.
3. Zhao M, Harris SE, Horn D, Geng Z, Nishimura R, Mundy GR, Chen D 2002 Bone morphogenetic protein receptor signaling is necessary for normal murine postnatal bone formation. J Cell Biol **157:**1049–1060.
4. Giannoudis PV, Kanakaris NK, Einhorn TA 2007 Interaction of bone morphogenetic proteins with cells of the osteoclast lineage: Review of the existing evidence. Osteoporos Int **18:**1565–1581.
5. Mishina Y, Starbuck MW, Gentile MA, Fukuda T, Kasparcova V, Seedor JG, Hanks MC, Amling M, Pinero GJ, Harada S, Behringer RR 2004 Bone morphogenetic protein type IA receptor signaling regulates postnatal osteoblast function and bone remodeling. J Biol Chem **279:**27560–27566.
6. Abe E, Yamamoto M, Taguchi Y, Lecka-Czernik B, O'Brien CA, Economides AN, Stahl N, Jilka RL, Manolagas SC 2000 Essential requirement of BMPs-2/4 for both osteoblast and osteoclast formation in murine bone marrow cultures from adult mice: Antagonism by noggin. J Bone Miner Res **15:**663–673.
7. Itoh K, Udagawa N, Katagiri T, Iemura S, Ueno N, Yasuda H, Higashio K, Quinn JM, Gillespie MT, Martin TJ, Suda T, Takahashi N 2001 Bone morphogenetic protein 2 stimulates osteoclast differentiation and survival supported by receptor activator of nuclear factor-kappaB ligand. Endocrinology **142:** 3656–3662.
8. Kanatani M, Sugimoto T, Kaji H, Kobayashi T, Nishiyama K, Fukase M, Kumegawa M, Chihara K 1995 Stimulatory effect of bone morphogenetic protein-2 on osteoclast-like cell formation and bone-resorbing activity. J Bone Miner Res **10:**1681–1690.
9. Kaneko H, Arakawa T, Mano H, Kaneda T, Ogasawara A, Nakagawa M, Toyama Y, Yabe Y, Kumegawa M, Hakeda Y 2000 Direct stimulation of osteoclastic bone resorption by bone morphogenetic protein (BMP)-2 and expression of BMP receptors in mature osteoclasts. Bone **27:**479–486.
10. Okamoto M, Murai J, Yoshikawa H, Tsumaki N 2006 Bone morphogenetic proteins in bone stimulate osteoclasts and osteoblasts during bone development. J Bone Miner Res **21:**1022–1033.
11. Feeley BT, Krenek L, Liu N, Hsu WK, Gamradt SC, Schwarz EM, Huard J, Lieberman JR 2006 Overexpression of noggin inhibits BMP-mediated growth of osteolytic prostate cancer lesions. Bone **38:**154–166.
12. Nohe A, Keating E, Knaus P, Petersen NO 2004 Signal transduction of bone morphogenetic protein receptors. Cell Signal **16:**291–299.
13. Xiao G, Gopalakrishnan R, Jiang D, Reith E, Benson MD, Franceschi RT 2002 Bone morphogenetic proteins, extracellular matrix, and mitogen-activated kinase signaling pathways are required for osteoblast-specific gene expression and differentiation in MC3T3-E1 cells. J Bone Miner Res **17:**101–110.
14. Balemans W, Van Hul W 2002 Extracellular regulation of BMP signaling in vertebrates: A cocktail of modulators. Dev Biol **250:**231–250.
15. Gazzerro E, Canalis E 2006 Bone morphogenetic proteins and their antagonists. Rev Endocr Metab Disord **7:**51–65.
16. Ebisawa T, Fukuchi M, Murakami G, Chiba T, Tanaka K, Imamura T, Miyazono K 2001 Smurf1 interacts with transforming growth factor-beta type I receptor through Smad7 and induces receptor degradation. J Biol Chem **276:**12477–12480.
17. Itoh F, Asao H, Sugamura K, Heldin CH, ten Dijke P, Itoh S 2001 Promoting bone morphogenetic protein signaling through negative regulation of inhibitory Smads. EMBO J **20:**4132–4142.
18. Lo RS, Massague J 1999 Ubiquitin-dependent degradation of TFG-beta activated Smad2. Nat Cell Biol **1:**472–478.
19. Abe E 2006 Function of BMPs and BMP antagonists in adult bone. Ann N Y Acad Sci **1068:**41–53.
20. Gazzerro E, Deregowski V, Vaira S, Canalis E 2005 Overexpression of twisted gastrulation inhibits bone morphogenetic protein action and prevents osteoblast cell differentiation in vitro. Endocrinology **146:**3875–3882.
21. Mason ED, Konrad KD, Webb CD, Marsh JL 1994 Dorsal midline fate in Drosophila embryos requires twisted gastrulation, a gene encoding a secreted protein related to human connective tissue growth factor. Genes Dev **8:**1489–1501.
22. Petryk A, Shimmi O, Jia X, Carlson AE, Tervonen L, Jarcho MP, O'Connor MB, Gopalakrishnan R 2005 Twisted gastrulation and chordin inhibit differentiation and mineralization in MC3T3-E1 osteoblast-like cells. Bone **36:**617–626.
23. Larrain J, Oelgeschlager M, Ketpura NI, Reversade B, Zakin L, De Robertis EM 2001 Proteolytic cleavage of Chordin as a switch for the dual activities of Twisted gastrulation in BMP signaling. Development **128:**4439–4447.
24. Oelgeschlager M, Larrain J, Geissert D, De Robertis EM 2000 The evolutionarily conserved BMP-binding protein Twisted gastrulation promotes BMP signalling. Nature **405:**757–763.
25. Oelgeschlager M, Reversade B, Larrain J, Little S, Mullins MC, De Robertis EM 2003 The pro-BMP activity of Twisted gastrulation is independent of BMP binding. Development **130:**4047–4056.
26. Ross JJ, Shimmi O, Vilmos P, Petryk A, Kim H, Gaudenz K, Hermanson S, Ekker SC, O'Connor MB, Marsh JL 2001 Twisted gastrulation is a conserved extracellular BMP antagonist. Nature **410:**479–483.
27. Scott IC, Blitz IL, Pappano WN, Maas SA, Cho KW, Greenspan DS 2001 Homologues of Twisted gastrulation are extracellular cofactors in antagonism of BMP signalling. Nature **410:**475–478.
28. Blitz IL, Cho KW, Chang C 2003 Twisted gastrulation loss-of-function analyses support its role as a BMP inhibitor during early Xenopus embryogenesis. Development **130:**4975–4988.
29. Petryk A, Anderson RM, Jarcho MP, Leaf I, Carlson CS, Klingensmith J, Shawlot W, O'Connor MB 2004 The mammalian twisted gastrulation gene functions in foregut and craniofacial development. Dev Biol **267:**374–386.
30. Mackenzie B, Wolff R, Lowe N, Billington CJ, Peterson A, Schmidt B, Graf D, Mina M, Gopalakrishnan R, Petryk A 2009 Twisted gastrulation limits apoptosis in the distal region of the mandibular arch in mice. Dev Biol **328:**13–23.
31. McCauley LK, Koh AJ, Beecher CA, Cui Y, Rosol TJ, Franceschi RT 1996 PTH/PTHrP receptor is temporally regulated during osteoblast differentiation and is associated with collagen synthesis. J Cell Biochem **61:**638–647.
32. Sharma SM, Bronisz A, Hu R, Patel K, Mansky KC, Sif S, Ostrowski MC 2007 MITF and PU.1 recruit p38 MAPK and NFATc1 to target genes during osteoclast differentiation. J Biol Chem **282:**15921–15929.

33. Wikesjo UM, Susin C, Qahash M, Polimeni G, Leknes KN, Shanaman RH, Prasad HS, Rohrer MD, Hall J 2006 The critical-size supraalveolar peri-implant defect model: Characteristics and use. J Clin Periodontol **33:**846–854.
34. Abramoff MD, Magehlaes PJ, Ram SJ 2004 Image processing with Image J. Biophotonics Int **11:**36–42.
35. Rozen S, Skaletsky H 2000 Primer3 on the WWW for general users and for biologist programmers. Methods Mol Biol **132:**365–386.
36. Hotokezaka H, Sakai E, Ohara N, Hotokezaka Y, Gonzales C, Matsuo K, Fujimura Y, Yoshida N, Nakayama K 2007 Molecular analysis of RANKL-independent cell fusion of osteoclast-like cells induced by TNF-alpha, lipopolysaccharide, or peptidoglycan. J Cell Biochem **101:**122–134.
37. Pham L, Purcell P, Morse L, Stashenko P, Battaglino RA 2007 Expression analysis of nha-oc/NHA2: A novel gene selectively expressed in osteoclasts. Gene Expr Patterns **7:**846–851.
38. Gazzerro E, Deregowski V, Stadmeyer L, Gale NW, Economides AN, Canalis E 2006 Twisted gastrulation, a bone morphogenetic protein agonist/antagonist, is not required for postnatal skeletal function. Bone **39:**1252–1260.
39. Yagi M, Miyamoto T, Sawatani Y, Iwamoto K, Hosogane N, Fujita N, Morita K, Ninomiya K, Suzuki T, Miyamoto K, Oike Y, Takeya M, Toyama Y, Suda T 2005 DC-STAMP is essential for cell-cell fusion in osteoclasts and foreign body giant cells. J Exp Med **202:**345–351.
40. Boyle WJ, Simonet WS, Lacey DL 2003 Osteoclast differentiation and activation. Nature **423:**337–342.
41. Zimmerman LB, De Jesus-Escobar JM, Harland RM 1996 The Spemann organizer signal noggin binds and inactivates bone morphogenetic protein 4. Cell **86:**599–606.
42. Garimella R, Tague SE, Zhang J, Belibi F, Nahar N, Sun BH, Insogna K, Wang J, Anderson HC 2008 Expression and synthesis of bone morphogenetic proteins by osteoclasts: A possible path to anabolic bone remodeling. J Histochem Cytochem **56:**569–577.
43. Nosaka T, Morita S, Kitamura H, Nakajima H, Shibata F, Morikawa Y, Kataoka Y, Ebihara Y, Kawashima T, Itoh T, Ozaki K, Senba E, Tsuji K, Makishima F, Yoshida N, Kitamura T 2003 Mammalian twisted gastrulation is essential for skeleto-lymphogenesis. Mol Cell Biol **23:**2969–2980.

Received in original form September 23, 2008; revised form March 8, 2009; accepted May 1, 2009.